

Electronic Supplementary Information

Nitrogen as a pnicogen?: Evidence for π -hole driven novel pnicogen bonding interactions in nitromethane-ammonia aggregates using matrix isolation infrared spectroscopy and ab initio computations

Swaroop Chandra, B. Suryaprasad, N. Ramanathan* and K. Sundararajan

Homi Bhabha National Institute, Materials Chemistry & Metal Fuel Cycle Group,
Indira Gandhi Center for Atomic Research, Kalpakkam – 603102, Tamil Nadu, India

S1 Computed shifts associated with selected modes of vibration from harmonic frequency calculations using various functionals.

Table S1. Computed wavenumbers associated with selected modes of vibration of NH₃ and NMeth submolecules, within heterodimers NAM I and NAM II, at CCSD level of theory with aug-cc-pVDZ basis set.

CCSD/aug-cc-pVDZ	Computed Wavenumber (Shift) cm ⁻¹	Intensity(km mol ⁻¹)
NH₃		
N-H bend (ν ₂)	1069.6	125
NM		
C-N stretch (ν ₁₃) ^[1,2]	1477.3	57
O=N=O stretch (ν ₇) ^[1,2]	1667.9	378
NM – AM I ΔE^a = 0 kcal mol⁻¹		
N-H bend	1122.2 (+52.6)	139
C-N stretch	1484.7(+7.4)	37
O=N=O stretch	1666.4 (-1.5)	296
NM – AM II ΔE^a = 1.77 kcal mol⁻¹		
N-H bend	1116.7 (+47.1)	138
C-N stretch	1480.8 (+3.5)	47
O=N=O stretch	1657.0 (-10.9)	371

^aInclusive of ZPE corrections

Table S2. Computed wavenumbers associated with selected modes of vibration of NH₃ and NMeth submolecules, within heterodimers NAM I, NAM II and NAM*, at MP2 level of theory with aug-cc-pVDZ basis set.

MP2/aug-cc-pVDZ	Computed Wavenumber (Shift) cm ⁻¹	Intensity(km mol ⁻¹)
NH₃		
N-H bend (ν ₂)	1042.8	132
NM		
C-N stretch (ν ₁₃) ^[1,2]	1420.6	36
O=N=O stretch (ν ₇) ^[1,2]	1760.5	156
NM – AM I		
N-H bend	1100.8 (+58.0)	144
C-N stretch	1429.9 (+9.3)	37
O=N=O stretch	1756.1 (-4.4)	136
NM – AM*		
N-H bend	1098.3 (+55.5)	147
C-N stretch	1431.8 (+11.2)	37
O=N=O stretch	1758.0 (-2.5)	135
NM – AM II		
N-H bend	1094.4 (+51.6)	144
C-N stretch	1425.2 (+4.6)	40
O=N=O stretch	1751.0 (-9.5)	166

Table S3. Computed wavenumbers associated with selected modes of vibration of NH₃ and NMeth submolecules, within heterodimers NAM I and NAM II, at MP4 level of theory with aug-cc-pVDZ basis set.

MP4/aug-cc-pVDZ	Computed Wavenumber (Shift) cm ⁻¹
NH₃	
N-H bend (ν_2)	1068.5
NM	
C-N stretch (ν_{13}) ^[1,2]	1363.2
O=N=O stretch (ν_7) ^[1,2]	1615.4
NM – AM I $\Delta E^a = 0$ kcal mol⁻¹	
N-H bend	1120.4(+51.9)
C-N stretch	1370.7 (+7.5)
O=N=O stretch	1609.8 (-5.6)
NM – AM II $\Delta E^a = 2.12$ kcal mol⁻¹	
N-H bend	1113.2 (+44.7)
C-N stretch	1363.0 (-0.2)
O=N=O stretch	1607.4 (-8.0)

^aInclusive of ZPE corrections

Table S4. Computed wavenumbers associated with selected modes of vibration of NH₃ and NMeth submolecules, within heterodimers NAM I, NAM II and NAM*, at B3LYP-GD3 level of theory with aug-cc-pVDZ basis set.

B3LYP/aug-cc-pVDZ	Computed Wavenumber (Shift) cm ⁻¹	Intensity(km mol ⁻¹)
NH₃		
N-H bend (ν_2)	1019.7	134
NM		
C-N stretch (ν_{13}) ^[1,2]	1431.9	64
O=N=O stretch (ν_7) ^[1,2]	1631.8	331
NM – AM I $\Delta E^a = 0$ kcal mol⁻¹		
N-H bend	1072.1(+52.4)	146
C-N stretch	1437.1 (+5.2)	305
O=N=O stretch	1616.6 (-15.2)	53
NM – AM* $\Delta E^a = 0.57$ kcal mol⁻¹		
N-H bend	1068.6 (+48.9)	149
C-N stretch	1439.2 (+7.3)	56
O=N=O stretch	1616.6 (-15.2)	308
NM – AM II $\Delta E^a = 1.91$ kcal mol⁻¹		
N-H bend	1068.7 (+49.0)	149
C-N stretch	1435.1 (+3.2)	48
O=N=O stretch	1623.4 (-8.4)	331

^aInclusive of ZPE corrections

Table S5. Computed wavenumbers associated with selected modes of vibration of NH₃ and NMeth submolecules, within heterodimers NAM I, NAM II and NAM*, at B2PLYP level of theory with aug-cc-pVDZ basis set.

B2PLYP/aug-cc-pVDZ	Computed Wavenumber (Shift) cm ⁻¹	Intensity(km mol ⁻¹)
NH₃		
N-H bend (ν₂)	1034.2	134
NM		
C-N stretch (ν₁₃)^[1,2]	1395.6	50
O=N=O stretch (ν₇)^[1,2]	1616.3	256
NM – AM I ΔE^a = 0 kcal mol⁻¹		
N-H bend	1092.0 (57.8)	145
C-N stretch	1418.5 (22.9)	34
O=N=O stretch	1607.2 (-9.1)	259
NM – AM* ΔE^a = 0.45 kcal mol⁻¹		
N-H bend	1087.9 (+53.7)	149
C-N stretch	1400.8 (+5.2)	35
O=N=O stretch	1607.6 (-8.7)	263
NM – AM II ΔE^a = 1.91 kcal mol⁻¹		
N-H bend	1095.6 (+61.4)	145
C-N stretch	1414.0 (+18.4)	47
O=N=O stretch	1607.0 (-9.3)	261

^aInclusive of ZPE corrections

S2 Coordinates and images of optimized geometries obtained at various levels of theory.

Coordinates of 1:1::NM:AM geometries at MP2/aug-cc-pVDZ

NM-AM I

7	-2.210260000	-0.201459000	0.000429000
1	-3.192779000	-0.475578000	0.000086000
1	-2.082150000	0.401686000	-0.813856000
1	-2.082872000	0.402599000	0.814145000
6	0.907672000	-1.278831000	0.000261000
1	1.451657000	-1.542924000	-0.912554000
1	1.452137000	-1.542280000	0.912970000
1	-0.105032000	-1.703701000	0.000671000
7	0.706117000	0.197387000	-0.000157000
8	0.602088000	0.759710000	-1.098817000
8	0.603164000	0.760500000	1.098201000

NM-AM II

7	3.402574000	0.001224000	0.009561000
1	3.800535000	0.716887000	0.618924000
1	3.804341000	0.168469000	-0.913729000
1	3.796880000	-0.885005000	0.327391000
6	0.226781000	0.013898000	-0.028765000
1	0.562973000	-0.794611000	-0.684595000
1	0.556317000	0.998200000	-0.371108000
1	0.566018000	-0.174833000	0.996622000
7	-1.266734000	0.000370000	-0.009290000
8	-1.821145000	-1.107291000	0.012066000
8	-1.853683000	1.091835000	0.012582000

NM-AM*

7	2.178375000	0.167723000	-0.001499000
1	3.152856000	0.470038000	0.009384000
1	2.077634000	-0.435963000	-0.819339000
1	2.061517000	-0.443173000	0.808838000
6	-0.845273000	1.295391000	-0.000448000
1	-0.372807000	1.680672000	0.907379000
1	-0.373576000	1.679395000	-0.909216000
1	-1.926456000	1.489814000	-0.000160000
7	-0.678037000	-0.185604000	0.000449000
8	-0.626153000	-0.754658000	1.099112000
8	-0.630085000	-0.756338000	-1.097469000

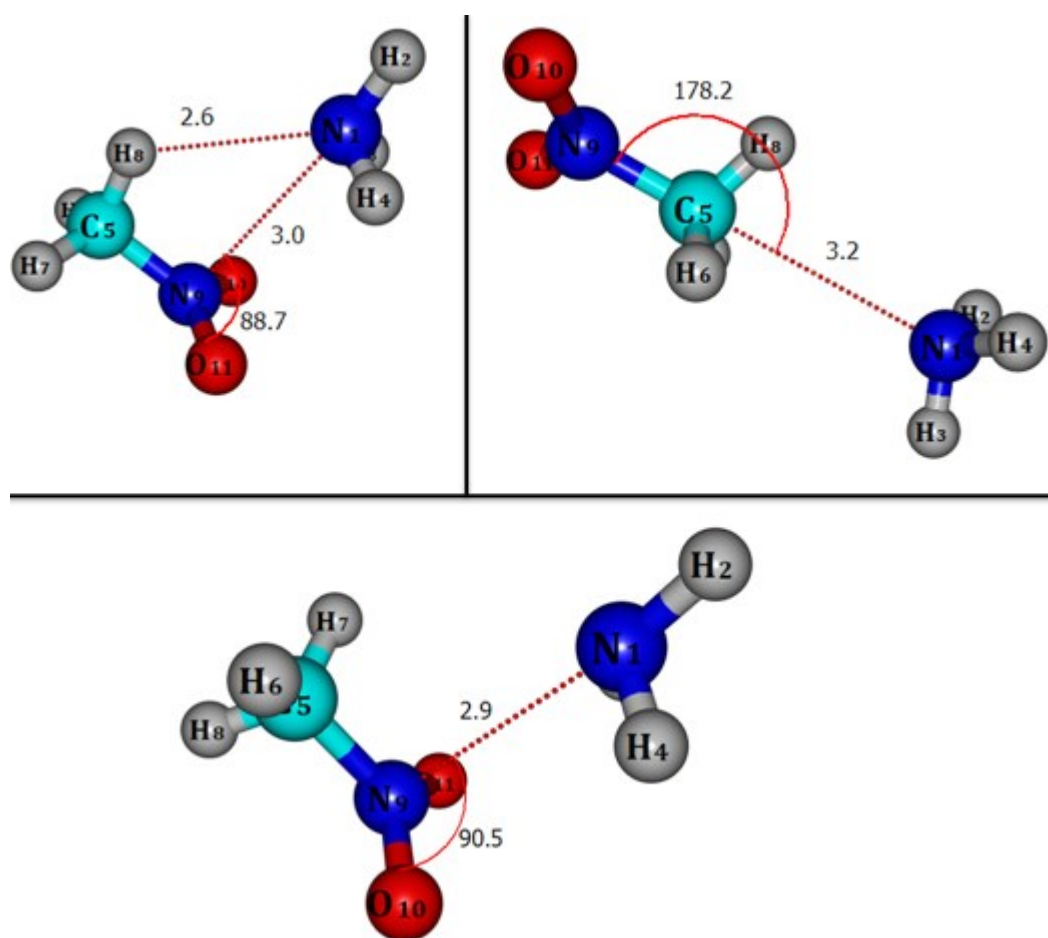


Figure S1. Optimized geometries on PES of 1:1::NM:AM at MP2/aug-cc-pVTZ

Coordinates of 1:1::NM:AM geometries at MP2/aug-cc-pVTZ

NM-AM I

7	-2.217564000	0.198826000	-0.000419000
1	-3.189627000	0.482105000	-0.000151000
1	-2.086255000	-0.395099000	0.810557000
1	-2.086946000	-0.395890000	-0.810924000
6	0.911746000	1.269572000	-0.000287000
1	1.449897000	1.532464000	0.902526000
1	1.450311000	1.531864000	-0.903026000
1	-0.088964000	1.694525000	-0.000649000
7	0.707133000	-0.197375000	0.000159000
8	0.602908000	-0.754438000	1.091296000
8	0.603858000	-0.755257000	-1.090645000

NM-AM II

7	-3.444076000	-0.001852000	0.000010000
1	-3.836177000	-0.465723000	0.810667000
1	-3.832434000	-0.469127000	-0.810497000
1	-3.824759000	0.936863000	-0.002832000
6	-0.205885000	-0.032026000	0.000593000
1	-0.545053000	0.494670000	-0.884075000
1	-0.527785000	-1.064227000	0.001385000
1	-0.544521000	0.495993000	0.884665000
7	1.278461000	-0.000214000	0.000045000
8	1.808671000	1.108908000	-0.000195000
8	1.879497000	-1.074137000	-0.000212000

NM-AM *

7	2.192786000	0.179112000	-0.001041000
1	3.163838000	0.465999000	0.009894000
1	2.073117000	-0.411345000	-0.816414000
1	2.057673000	-0.421162000	0.804728000
6	-0.868797000	1.280713000	-0.000017000
1	-0.409629000	1.671225000	0.898737000
1	-0.406710000	1.671031000	-0.897372000
1	-1.941361000	1.457684000	-0.001875000
7	-0.679760000	-0.189123000	0.000335000
8	-0.618165000	-0.752623000	1.091229000
8	-0.621251000	-0.753331000	-1.090310000

Table S6. Relative and binding energies (all in kcal mol⁻¹), of NM-AM I and II, inclusive of zero point energies at MP2/aug-cc-pVTZ level.

Heterodimer	Relative Energy	ZPE Corr Binding Energy
NM-AM I	0	-4.34
NM-AM II	1.18	-2.16

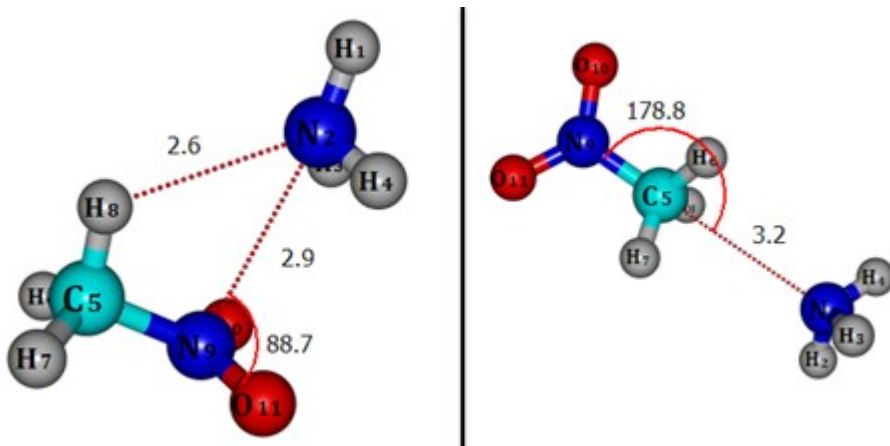


Figure S2. Optimized geometries of minima on PES of 1:1::NM:AM at MP4/aug-cc-pVDZ

Coordinates of 1:1::NM:AM geometries at MP4/aug-cc-pVDZ

NM-AM I

1	-3.176771000	0.494547000	0.079212000
7	-2.193585000	0.222177000	-0.004158000
1	-2.012368000	-0.419721000	0.773576000
1	-2.130121000	-0.351858000	-0.850178000
6	0.930328000	1.280031000	-0.002496000
1	1.478661000	1.527160000	0.916846000
1	1.491249000	1.533399000	-0.912598000
1	-0.076072000	1.727554000	-0.010299000
7	0.697513000	-0.205636000	0.000933000
8	0.577915000	-0.765688000	1.106531000
8	0.586580000	-0.772694000	-1.101408000

NM-AM II

7	-3.393937000	-0.001928000	0.007259000
1	-3.797402000	-0.719674000	0.615958000
1	-3.802667000	-0.165683000	-0.916938000
1	-3.791277000	0.885069000	0.328882000
6	-0.238172000	-0.009833000	-0.022981000
1	-0.572835000	0.803028000	-0.679941000
1	-0.571371000	-0.996604000	-0.365862000
1	-0.569873000	0.180008000	1.008176000
7	1.267813000	-0.000937000	-0.009194000
8	1.825225000	1.112879000	0.009956000
8	1.851940000	-1.101265000	0.010189000

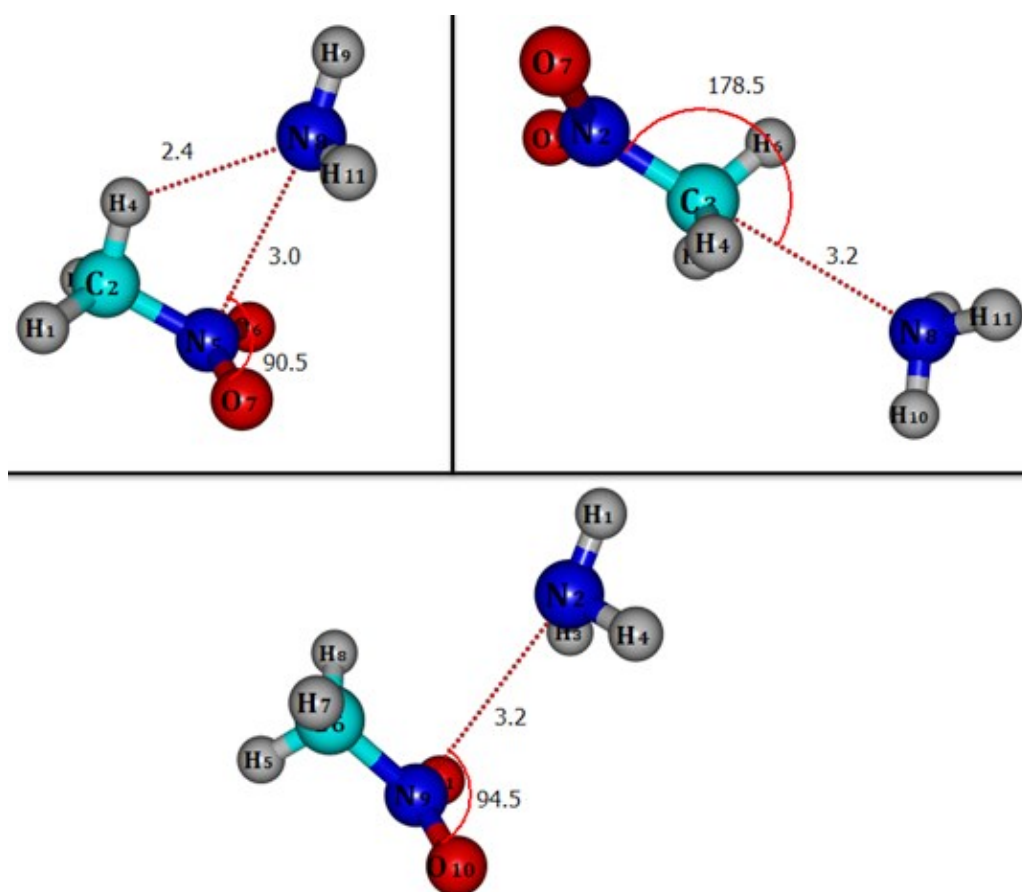


Figure S3. Optimized geometries on PES of 1:1::NM:AM at CCSD/aug-cc-pVDZ

Coordinates of 1:1::NM:AM geometries at CCSD/aug-cc-pVDZ

NM-AM I

7	2.253269000	0.168730000	0.000013000
1	3.233359000	0.454636000	-0.000466000
1	2.132802000	-0.437296000	-0.814334000
1	2.133479000	-0.436880000	0.814769000
6	-0.874324000	1.295572000	0.000007000
1	-1.410216000	1.575732000	-0.914464000
1	-1.410299000	1.575707000	0.914437000
1	0.153884000	1.684606000	0.000060000
7	-0.722643000	-0.192489000	-0.000003000
8	-0.643828000	-0.751468000	-1.088208000
8	-0.643853000	-0.751484000	1.088193000

NM-AM II

7	-3.404002000	-0.000921000	0.009999000
1	-3.802595000	-0.718085000	0.619099000
1	-3.807243000	-0.166709000	-0.914172000
1	-3.798551000	0.885788000	0.329826000
6	-0.225874000	-0.014681000	-0.030386000
1	-0.560709000	0.796330000	-0.686080000
1	-0.554471000	-1.000017000	-0.374693000
1	-0.563013000	0.172905000	0.997511000
7	1.272190000	-0.000474000	-0.008695000
8	1.819040000	1.097239000	0.012315000
8	1.851523000	-1.081285000	0.012897000

NM-AM *

1	-3.369819000	0.211641000	0.249057000
7	-2.411137000	-0.022588000	-0.029822000
1	-2.018831000	-0.623669000	0.702515000
1	-2.526350000	-0.647981000	-0.837806000
1	1.596950000	1.760438000	0.119834000
6	0.579449000	1.386036000	-0.034326000
1	0.173924000	1.802833000	-0.972965000
1	0.067873000	1.704727000	0.882217000
7	0.810995000	-0.146819000	-0.000332000
8	0.894422000	-0.728955000	-1.079832000
8	0.830646000	-0.688339000	1.114105000

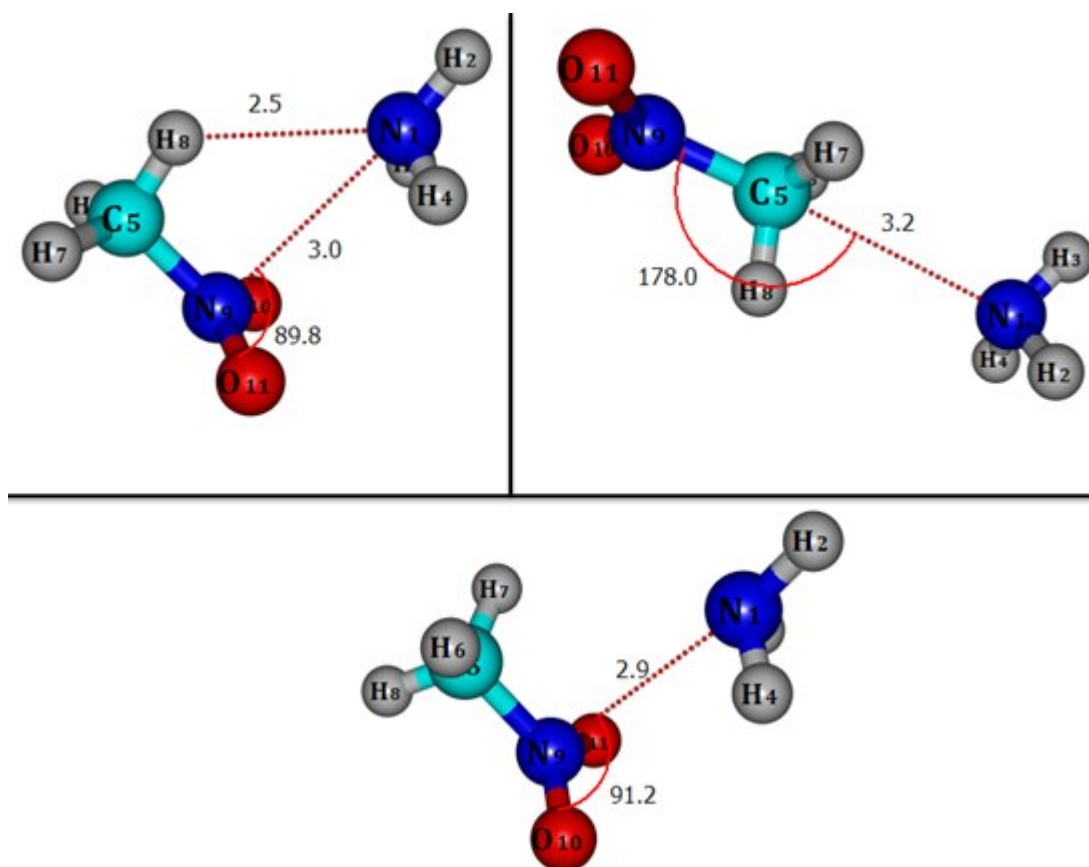


Figure S4. Optimized geometries on PES of 1:1::NM:AM at B3LYP-GD3/aug-cc-pVDZ

Coordinates of 1:1::NM:AM geometries at B3LYP-GD3/aug-cc-pVDZ

NM-AM I

7	-2.253962000	0.147318000	-0.000217000
1	-3.242956000	0.386583000	0.000253000
1	-2.091660000	-0.442797000	0.814476000
1	-2.092422000	-0.442704000	-0.815126000
6	0.835679000	1.307235000	-0.000066000
1	1.355987000	1.607620000	0.912097000
1	1.356204000	1.607438000	-0.912162000
1	-0.203970000	1.656525000	-0.000214000
7	0.727933000	-0.184553000	0.000076000
8	0.661353000	-0.747078000	1.087528000
8	0.662015000	-0.747350000	-1.087271000

NM-AM II

7	-3.398877000	-0.000812000	0.011239000
1	-3.787397000	-0.714410000	0.625935000
1	-3.793708000	-0.172763000	-0.912088000
1	-3.783333000	0.888716000	0.325811000
6	-0.230262000	-0.016873000	-0.034475000
1	-0.566318000	0.788892000	-0.689198000
1	-0.560527000	-1.000003000	-0.369774000
1	-0.567631000	0.176807000	0.988124000
7	1.269481000	-0.000479000	-0.008550000
8	1.816168000	1.097313000	0.013348000
8	1.852115000	-1.079434000	0.014054000

NM-AM *

7	2.212562000	0.151020000	-0.000114000
1	3.194130000	0.419599000	0.017374000
1	2.081337000	-0.433855000	-0.824166000
1	2.057661000	-0.453728000	0.805327000
6	-0.827834000	1.305294000	0.000212000
1	-0.352065000	1.681276000	0.906830000
1	-0.351617000	1.681502000	-0.906076000
1	-1.904124000	1.513696000	-0.000076000
7	-0.690280000	-0.185052000	0.000031000
8	-0.650529000	-0.750233000	1.087156000
8	-0.651258000	-0.750021000	-1.087144000

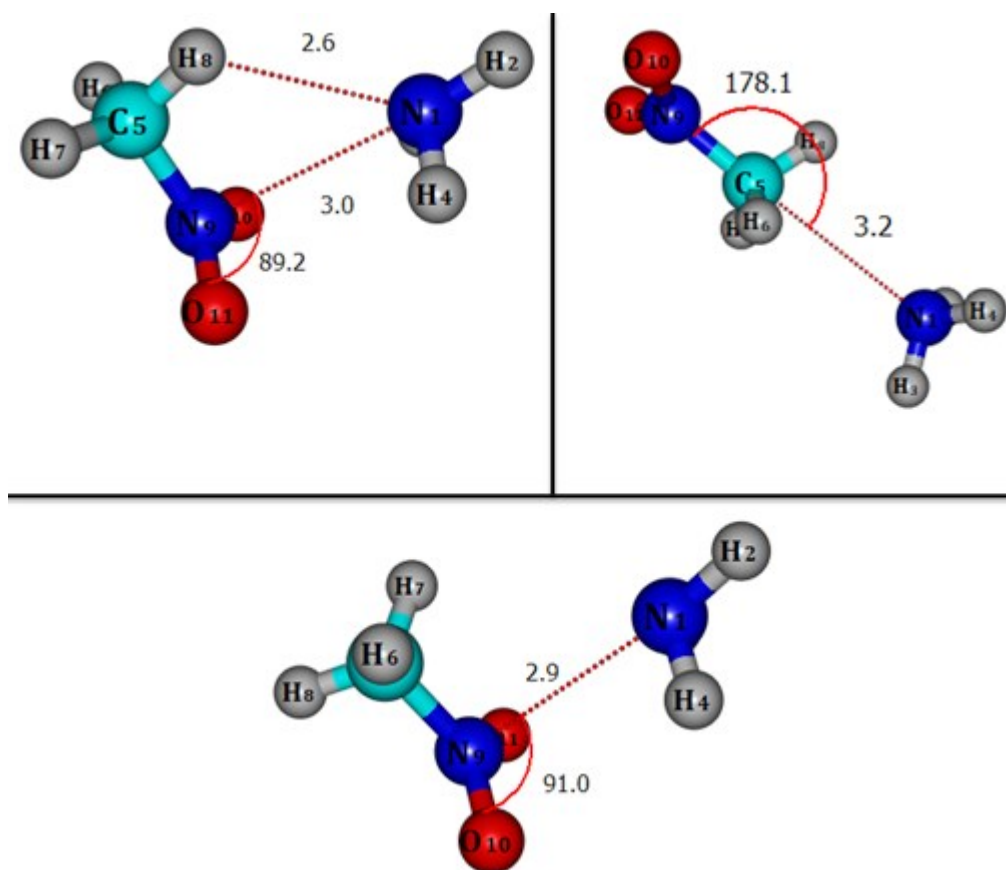


Figure S5. Optimized geometries on PES of 1:1::NM:AM at B2PLYP-GD3/aug-cc-pVDZ

Coordinates of 1:1::NM:AM geometries at B2PLYP-GD3/aug-cc-pVDZ

NM-AM I

7	-2.225563000	0.181312000	-0.000133000
1	-3.211864000	0.430885000	-0.000046000
1	-2.074876000	-0.413088000	0.813516000
1	-2.075077000	-0.413309000	-0.813657000
6	0.879485000	1.290695000	-0.000016000
1	1.413165000	1.568010000	0.911352000
1	1.413277000	1.567927000	-0.911344000
1	-0.143411000	1.683358000	-0.000094000
7	0.713512000	-0.193016000	0.000042000
8	0.623924000	-0.755304000	1.093524000
8	0.624354000	-0.755449000	-1.093398000

NM-AM II

7	-3.399602000	-0.001027000	0.010633000
1	-3.794344000	-0.715277000	0.620402000
1	-3.799879000	-0.168568000	-0.911033000
1	-3.790355000	0.884631000	0.328000000
6	-0.228478000	-0.015550000	-0.032372000
1	-0.563766000	0.791332000	-0.685322000
1	-0.557526000	-0.997319000	-0.371798000
1	-0.564999000	0.173838000	0.990533000
7	1.267613000	-0.000453000	-0.009187000
8	1.818069000	1.103106000	0.013024000
8	1.852639000	-1.086227000	0.013642000

NM-AM *

7	2.192580000	0.160212000	-0.000305000
1	3.169532000	0.444766000	0.012798000
1	2.073292000	-0.432638000	-0.820273000
1	2.055185000	-0.445729000	0.807204000
6	-0.837139000	1.300157000	-0.000051000
1	-0.364495000	1.680014000	0.906246000
1	-0.363878000	1.679882000	-0.906081000
1	-1.914702000	1.498149000	-0.000461000
7	-0.683020000	-0.185529000	0.000071000
8	-0.637025000	-0.752883000	1.093411000
8	-0.637853000	-0.753139000	-1.093097000

S2 Relevant delocalisations from NBO analysis

Table S7. Second order perturbation energies (E_2 , in kcal mol⁻¹) associated with characteristic intermolecular NBO delocalisations in NAM I along with their respective occupancies.

Donor	Acceptor	E_2	Occupancy ^a	
			Donor	Acceptor
lp(N1)	$\sigma^*(C5-H8)$	2.14	1.99175(1.99530)	0.00613(0.00446)
	$\sigma^*(C5-N9)$	0.13		0.04907(0.05057)
	$\pi^*(N9-O11)$			0.33
$\sigma(N1-H3)$		0.06		
$\pi(N9-O11)$	$\sigma^*(N1-H2)$	0.11	1.99396(1.99274)	0.00024(0.00001)
	$\sigma^*(N1-H4)$	0.15		0.00041(0.00001)
lp(O10)	$\sigma^*(N1-H3)$	0.22	1.50878(1.50774)	0.00042(0.00001)

^aOccupancy of NBO in the monomer shown within parenthesis

Table S8. Second order perturbation energies (E_2 , in kcal mol⁻¹) associated with characteristic intermolecular NBO delocalisations in NAM* along with their respective occupancies.

Donor	Acceptor	E_2	Occupancy ^a	
			Donor	Acceptor
lp(N1)	$\sigma^*(C5-H8)$	0.54	1.99286(1.99530)	0.00398(0.00446)
	$\sigma^*(C5-N9)$	0.22		0.04964(0.05057)
	$\pi^*(N9-O11)$			0.55
$\sigma(N1-H3)$		0.1		
$\pi(N9-O11)$	$\sigma^*(N1-H2)$	0.12	1.99334(1.99274)	0.00031(0.00001)
	$\sigma^*(N1-H4)$	0.13		0.00041(0.00001)
lp(O10)	$\sigma^*(N1-H3)$	0.21	1.50538(1.50774)	0.00036(0.00001)

^aOccupancy of NBO in the monomer shown within parenthesis

Table S9. Second order perturbation energies (E_2 , in kcal mol⁻¹) associated with characteristic intermolecular NBO delocalisations in N...N bonded 2:1::NH₃:NMeth heterotrimer along with their respective occupancies.

Donor	Acceptor	E_2	Occupancy ^a	
			Donor	Acceptor
lp(N1)	$\sigma^*(C5-H8)$	1.72	1.99237(1.99530)	0.00616(0.00446)
	$\sigma^*(C5-N9)$	0.11		0.04831(0.05057)
	$\pi^*(N9-O11)$	0.35		0.49776(0.50337)
$\sigma(N1-H3)$	$\pi^*(N9-O11)$	0.08	1.99859(1.99928)	
lp(N13)	$\sigma^*(C5-H8)$	0.41	1.99318(1.99530)	0.00616(0.00446)
	$\sigma^*(C5-N9)$	0.19		0.04831(0.05057)
	$\pi^*(N9-O11)$	0.56		0.49776(0.50337)
$\sigma(N13-H14)$	$\pi^*(N9-O11)$	0.11	1.99844(1.99928)	
$\pi(N9-O11)$	$\sigma^*(N1-H2)$	0.1	1.99325(1.99274)	0.00025(0.00001)
	$\sigma^*(N1-H4)$	0.15		0.00047(0.00001)
	$\sigma^*(N13-H12)$	0.15		0.00045(0.00001)
	$\sigma^*(N13-H15)$	0.11		0.00031(0.00001)
lp(O10)	$\sigma^*(N1-H3)$	0.24	1.51598(1.50774)	0.00050(0.00001)
	$\sigma^*(N13-H14)$	0.23		0.00046(0.00001)

^aOccupancy of NBO in the monomer shown within parenthesis

S3 Nitromethane – H₂O experiments

Table S10. Assignment of modes of vibration to new features observed in NMeth-H₂O co-deposition experiments

Computed Wavenumber (cm ⁻¹)		Experimental Wavenumber (cm ⁻¹)				Mode Assignment
ν	$\Delta\nu$	Ar		N ₂		
		ν	$\Delta\nu$	ν	$\Delta\nu$	
O-H Stretching						
3938.3 (67)	---	3756.4	---	3727.4	---	ν_3 of H ₂ O monomer ^[3]
3904.3 (139)	-38.0	3715.1	-41.3	3715.6/ 3706.2/ 3700.0	-20.1	Anti-symmetric O-H stretch in NMeth-H ₂ O
O=N=O Stretching						
1760.5(156)	---	1570.1	---	1572.7	---	ν_3 of NMeth monomer ^[1,2]
1748.6 (174)	-11.9	1564.1	-6.0	1568.4/ 1564.3	-6.4	O=N=O stretch in NMeth-H ₂ O

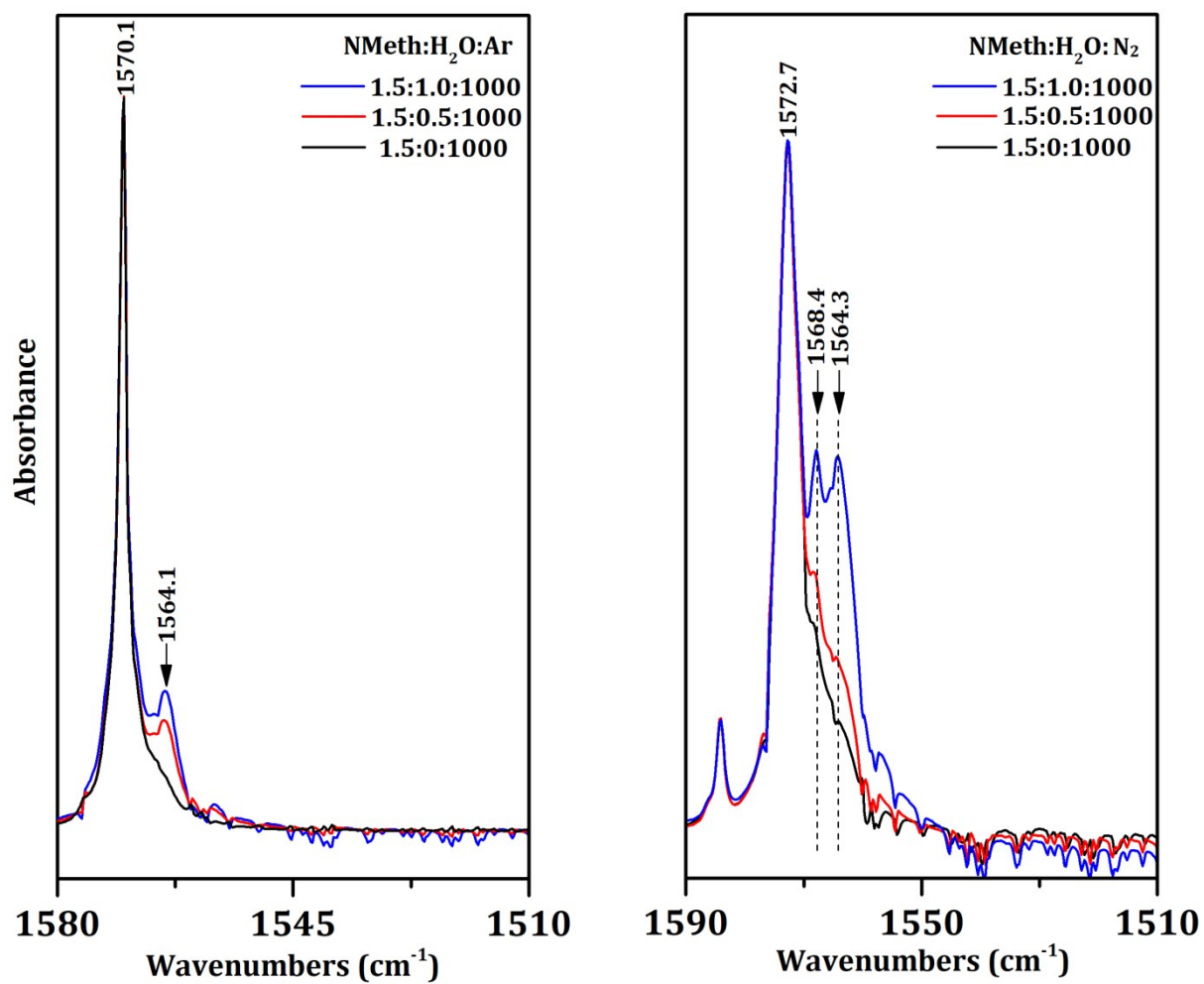


Figure S6. Infrared spectra of O=N=O stretching region of NMeth corresponding to the co-deposition experiments of H₂O and NMeth in Ar and N₂ matrix. All spectra were recorded at 12 K following a 15 minute annealing, at 35 K (Ar); at 32 K (N₂).

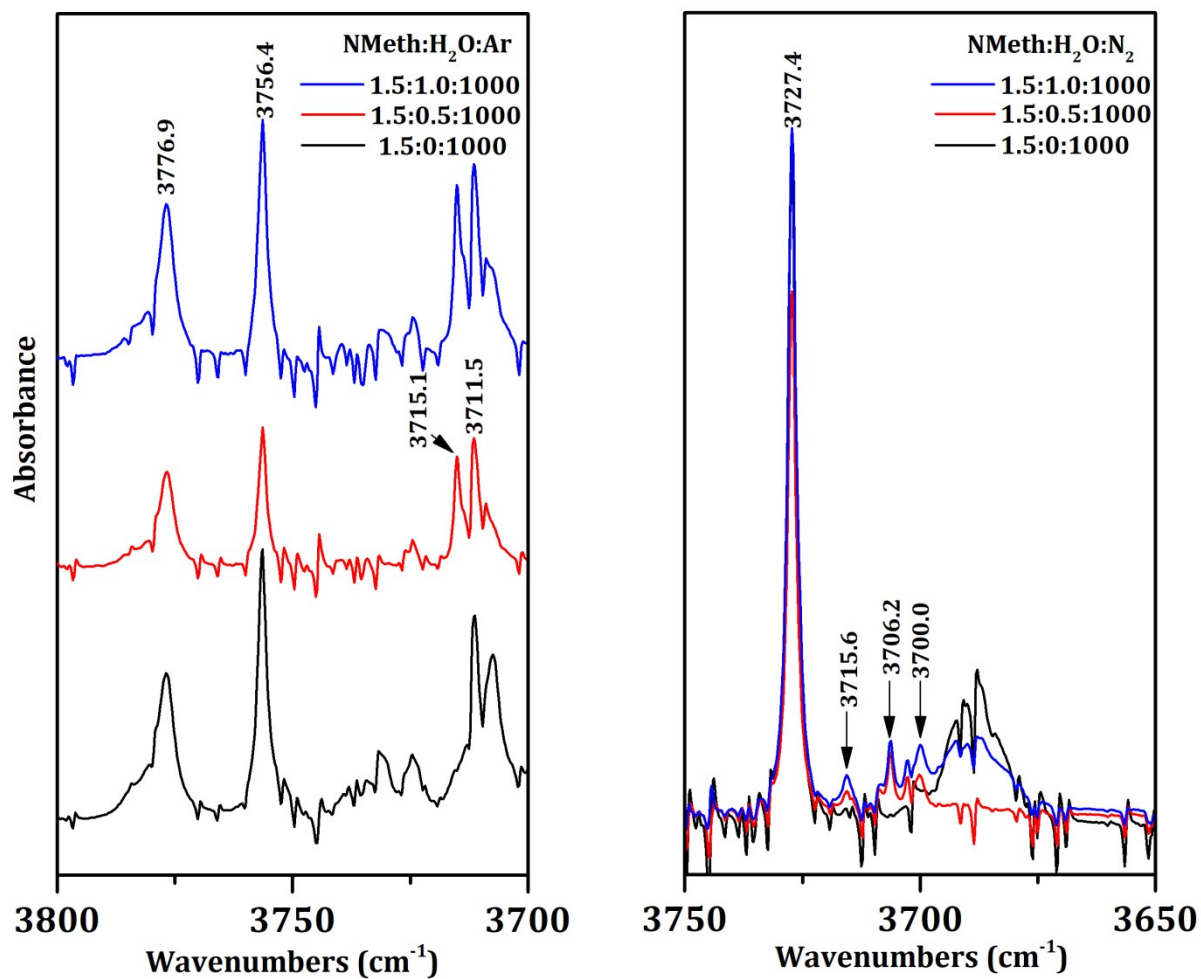


Figure S7. Infrared spectra of O-H stretching region of H₂O corresponding to the co-deposition experiments of H₂O and NMeth in Ar and N₂ matrix. All spectra were recorded at 12 K following a 15 minute annealing, at 35 K (Ar); at 32 K (N₂).

S4 Minima on the PES of NMeth:NH₃ heterotrimers

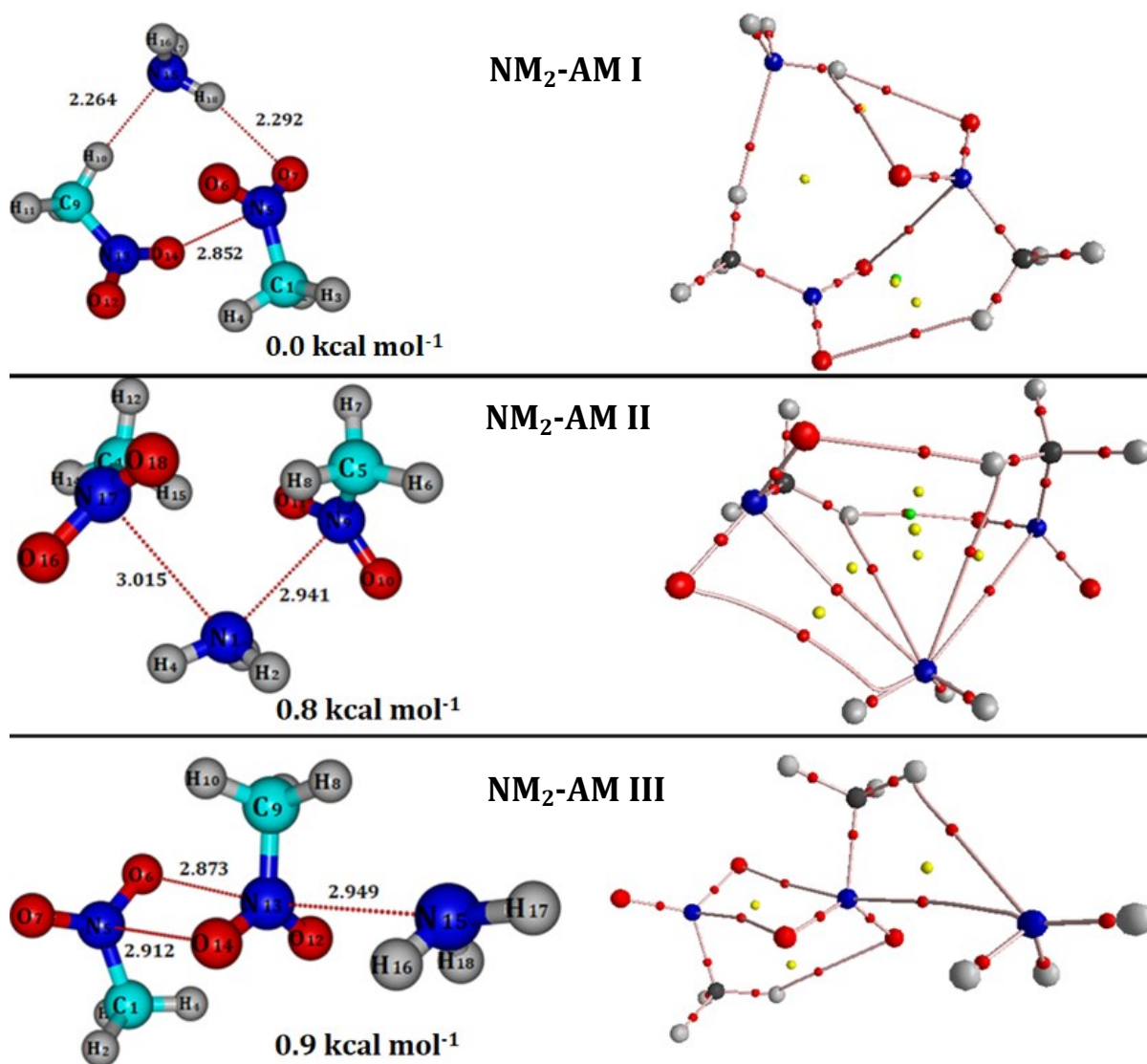


Figure S8. Optimized geometries corresponding to energetic minima on the PES of 2:1::NM:AM heterotrimer, with the respective energies relative to the global minimum.

Table S11. BSSE/ZPE (all in kcal mol⁻¹) corrected binding energies for 2:1::NM:AM heterotrimers

Heterotrimer	ZPE corrected	BSSE corrected
NM ₂ -AM I	-12.6	-15.4
NM ₂ -AM II	-11.8	-14.2
NM ₂ -AM III	-11.7	-14.1

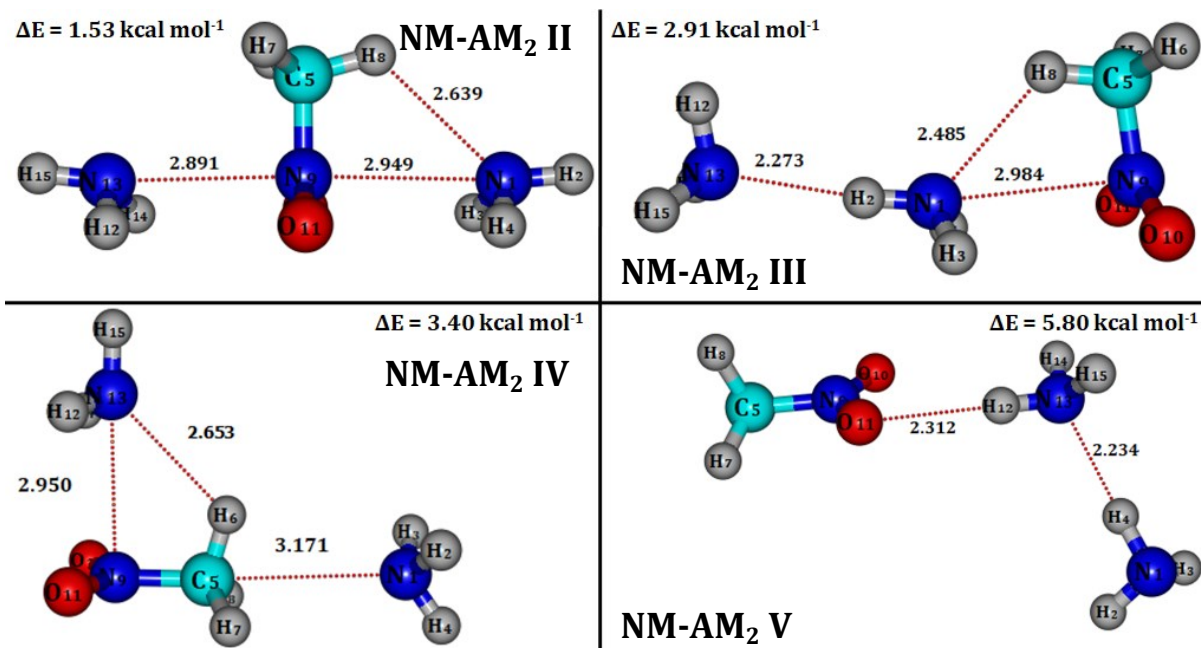


Figure S9. Optimized geometries corresponding to local minima on the PES of 1:2::NM:AM heterotrimer, with the respective energies relative to the global minimum.

Table S12. BSSE/ZPE (all in kcal mol⁻¹) corrected binding energies for 1:2::NM:AM heterotrimers

Heterotrimer	ZPE corrected	BSSE corrected
NM-AM ₂ I	-10.3	-13.8
NM-AM ₂ II	-8.8	-11.5
NM-AM ₂ III	-7.4	-10.2
NM-AM ₂ IV	-6.9	-9.1
NM-AM ₂ V	-4.5	-6.8

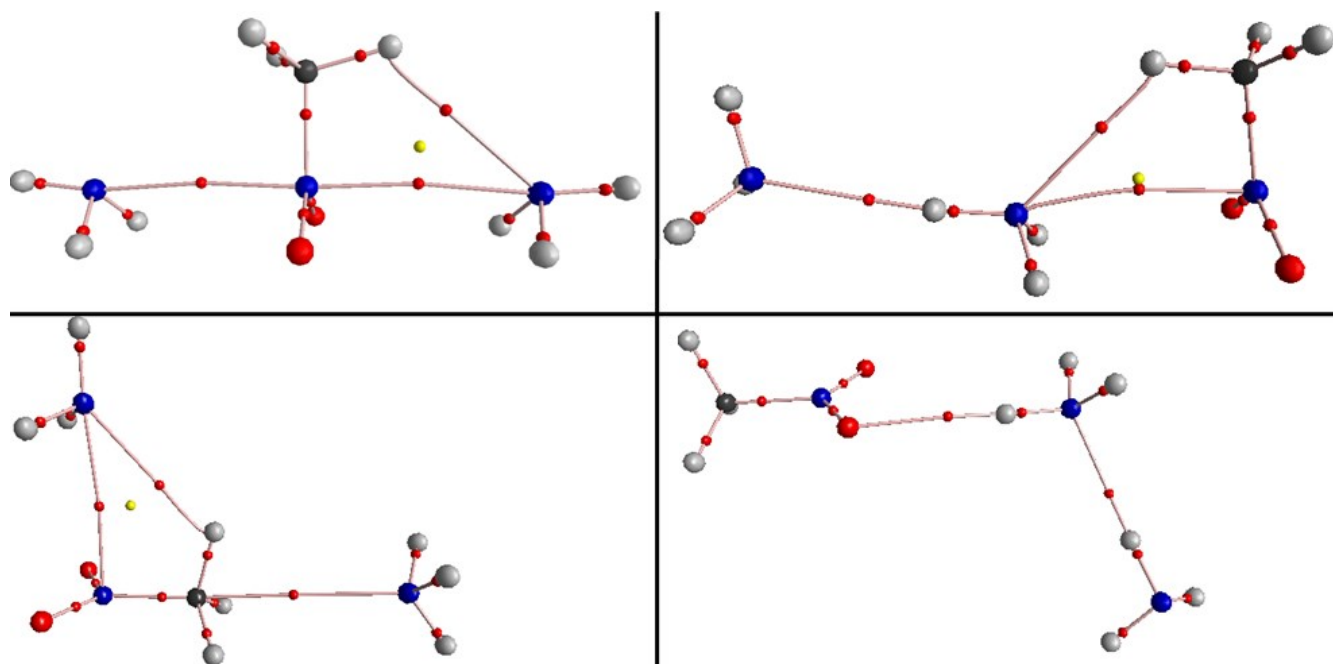


Figure S10. QTAIM plots of local minima on the PES of 1:2::NM:AM heterotrimers with BCPs in red and RCPs in yellow.

References:

- [1] F. D. Verderame, J. A. Lannon, L. E. Harris, W. G. Thomas, E. A. Lucia, *J. Chem. Phys.* **1972**, *56*, 2638–2648.
- [2] H. W. Brown, G. C. Pimentel, *J. Chem. Phys.* **1958**, *29*, 883–888.
- [3] G. P. Ayers, A. D. E. Pullin, *Spectrochim. Acta Part A Mol. Spectrosc.* **1976**, *32*, 1629–1639.
- [4] M. J. Frisch, G. W. Trucks, H. B. Schlegel, G. E. Scuseria, M. A. Robb, J. R. Cheeseman, G. Scalmani, V. Barone, B. Mennucci, G. A. Petersson, H. Nakatsuji, M. Caricato, X. Li, H. P. Hratchian, A. F. Izmaylov, J. Bloino, G. Zheng, J. L. Sonnenberg, M. Hada, M. Ehara, K. Toyota, R. Fukuda, J. Hasegawa, M. Ishida, T. Nakajima, Y. Honda, O. Kitao, H. Nakai, T. Vreven, J. A. Montgomery, Jr., J. E. Peralta, F. Ogliaro, M. Bearpark, J. J. Heyd, E. Brothers, K. N. Kudin, V. N. Staroverov, R. Kobayashi, J. Normand, K. Raghavachari, A. Rendell, J. C. Burant, S. S. Iyengar, J. Tomasi, M. Cossi, N. Rega, J. M. Millam, M. Klene, J. E. Knox, J. B. Cross, V. Bakken, C. Adamo, J. Jaramillo, R. Gomperts, R. E. Stratmann, O. Yazyev, A. J. Austin, R. Cammi, C. Pomelli, J. W. Ochterski, R. L. Martin, K. Morokuma, V. G. Zakrzewski, G. A. Voth, P. Salvador, J. J. Dannenberg, S. Dapprich, A. D. Daniels, O. Farkas, J. B. Foresman, J. V. Ortiz, J. Cioslowski and D. J. Fox, Gaussian 09, Revision D.01, Gaussian Inc., Wallingford CT, 2009.
- [5] T. Lu, F. Chen, *J. Comput. Chem.* **2012**, *33*, 580–592.
- [6] W. Humphrey, A. Dalke, K. Schulten, *J. Mol. Graph.* **1996**, *14*, 33–38.